Journal of Korea Robotics Society (2017) 12(1):078-085
https://doi.org/10.7746/jkros.2017.12.1.078 ISSN: 1975-6291 / eISSN: 2287-3961

3D 프린터 기반 수직형 마이크로 모션 스테이지의 최적설계

Optimal Design of 3D Printer based Piezo-driven Vertical Micro-positioning Stage

김 정 현[†]

Jung Hyun Kim[†]

Abstract This paper presents the development of a 3D printer based piezo-driven vertical micro-positioning stage. The stage consists of two flexure bridge structures which amplify and transfer the horizontal motion of the piezo-element into vertical motion of the end-effector. The stage is fabricated with ABS material using a precision 3D printer. This enables a one-body design eliminating the need for assembly, and significantly increases the freedom in design while shortening fabrication time. The design of the stage was optimized using response surface analysis method. Experimental results are presented which demonstrate 100nm stepping in the vertical out-of-plane direction. The results demonstrate the future possibilities of applying 3D printers and ABS material in fabricating linear driven motion stages.

Keywords 3D printer, piezo, motion stage, flexure hinge, flexure, motion control, ABS

1. Introduction

Many measurement and fabrication processes in state-of-the-art semiconductor manufacturing and nano-technology require motion control with near nanometer precision. At the same time, 3D printing is emerging as a game changer in many manufacturing areas such as aero-space, optics among many others. This paper presents a novel effort to develop a piezo-driven linear motion stage using 3D printing technology, which can possibly greatly decrease the cost and simplify the process of building stages.

Piezo-driven linear motion stages can perform various motions ranging from 1 to 6 degree-of-freedom depending on various design factors such as number of actuators used, the degree of motion amplification, etc. Previous work on 1 degree-of-freedom motion stages include inquiries into parallel mechanisms and monolithic structures [1,2], bridge-type flex hinges [3], 3D bridge type hinges [4], tilt tables using half-bridges [5] and etc. Further work on 2, 3 & 6 degree-of-freedom has also been done [6,7,8,15].

Recently, due to the advancement in 3D printer technology and its many advantages, 3D printing is gaining much interest not only in technology but also in general society. Advantages include simplified manufacturing processes, one body manufacturing eliminating the need for assembly, various materials and etc. As a result, governments in United States, United Kingdom, China and many other countries are leading various R&D efforts [9], while

Received : Oct. 29. 2016; Revised : Jan. 12. 2017; Accepted : Feb. 20. 2017
※This research was supported by Kyungsung University Research Grants in 2016
[†]Corresponding author: Mechatronics Engineering, Kyungsung University, 48434. 309, Suyeong-ro, Nam-gu, Busan, Republic of Korea (dwellnom@ksu.ac.kr)

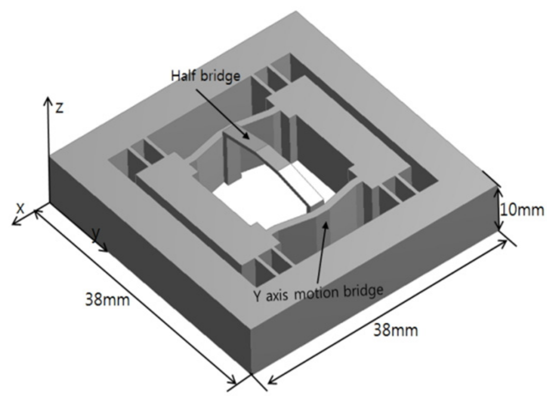

Fig. 1. Diagram of vertical micropositioning stage

industries such as automotive, aerospace, medicine, robotics, art, education and etc. are pursuing research into applying this emerging technology.

3D printers enable rapid prototyping of virtual 3D models drastically shortening design and fabrication time and is shown to increase the accuracy of design optimization [10]. In die casting, Kim et.al [11] has developed a novel rapid tooling process where a wax pattern fabricated with a 3D printer is used. In motion stages, Jung et.al [12] developed a micro-positioning stage using 3D printer.

This paper presents a 3D printer fabricated vertical-type piezo-driven linear motion stage employing two types of flexible bridge typed hinges (Fig. 1). Unlike previous stages which mostly use aluminum [4,5], we use ABS (Acrylonitrile - Butadiene - Styrene copolymer). Compared to previous materials, the stage structure exhibits significantly less structural stress which allows for more freedom of design. Furthermore, the required force to actuate the motion stage decreases. This relaxes power requirements for the piezoelectric element. Using a 3D printer, we simplified the manufacturing process, lowered costs and with ABS material created a more efficient stage.

2. Flexible Bridge-type Hinge

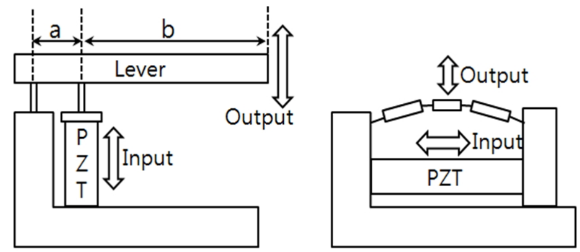

(a) Lever - type (b) Bridge - type

Fig. 2. Topology of amplification mechanism

2.1 Motion Amplification Structure

In general, when designing a flexure stage two types of motion amplification structures are employed: the lever type shown in Fig. 2-(a) and the bridge type shown in Fig. 2-(b). The lever type allows for a large amplification ratio (b/a) that is proportional to the length of the structure. However, the structural stress also increases proportionally. This renders the need for stronger materials. Overall, the lever-type is more appropriate for in-plane motion amplification. The bridge-type has a smaller symmetric form-factor allowing for a denser design and has better vibrational characteristics making it better for out-of-plane motion structures. In this paper, we are implementing out-of-plane motion, therefore, the bridge-type hinge is employed.

2.2 Bridge-type Flexure Hinge

Two types of flexure hinges have been designed. First, as shown in Fig. 3-(a), the bridge transforms the x-axis motion of the piezo-element into y-axis motion. Second, as shown in Fig. 3-(b), a half-bridge transforms the y-axis bridge motion into z-axis motion.

These two bridges have been used to design a dense structure which can transform x-axis motion into z-axis motion. Furthermore, stress concentration is avoided by avoiding a notch type hinge. Although this can lead decreased flexibility, it is beneficial for performance with regards to stress.

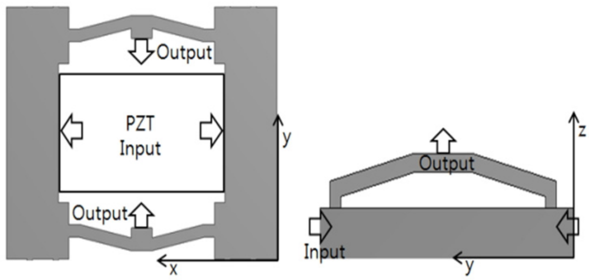

(a) Y axis motion bridge (b) Half - bridge

Fig. 3. Bridge mechanism

2.3 Amplification structure of Bridge-type Flexure Hinge

A kinematic model of bridge-type amplification mechanism can be expressed as Figure 4. Defining the velocity of point A and B,

$$V_A = \frac{\partial x}{\partial t} \quad (1)$$

$$V_B = \frac{\partial y}{\partial t} \quad (2)$$

Where ∂x is the displacement of the piezo-element and ∂y is the displacement of the bridge. Expressing equations (1) and (2) as an amplification ratio

$$V_A = \frac{\partial x}{\partial t} \quad (3)$$

$$V_B = \frac{\partial y}{e} \partial t \quad (4)$$

Where ∂x is the displacement of the piezo-element and ∂y is the displacement of the bridge. Expressing equations (3) and (4) as an amplification ratio,

$$D_{amp} = \frac{\partial y}{\partial x} = \frac{\partial y / \partial t}{\partial x / \partial t} = \frac{V_B}{V_A} \quad (5)$$

Defining O (Figure 4) as the instantaneous center of rotation of rigid body AB, as the instantaneous angular

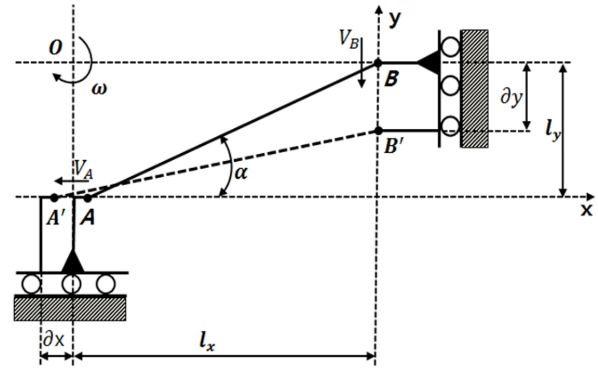

Fig. 4. Kinematic model of bridge-type amplification mechanism

velocity, velocity of A and B can be expressed as,

$$V_A = \omega \cdot l_x \quad (6)$$

$$V_B = \omega \cdot l_y \quad (7)$$

Expressing (6) and (7) as amplification ratio, the following equation is obtained,

$$D_{amp} = \frac{\omega \cdot l_y}{\omega \cdot l_x} = \frac{l_y}{l_x} = \cot\alpha \quad (8)$$

It is evident from the above equation that determines the amplification ratio, therefore is the critical design factor.

3. Design Optimization and Simulation

3.1 Design Optimization

The optimization method employed in this paper is Response surface analysis. For Design of Experiment (DOE) the Central Composite Design (CCD) was used. The design factor used is α (Fig. 4) of the Bridge-type flexure hinge, which has been shown to have a critical effect on the amplification ratio of the motion amplification structure.

Design variables θ_1, θ_2 (Fig. 5) which correspond to

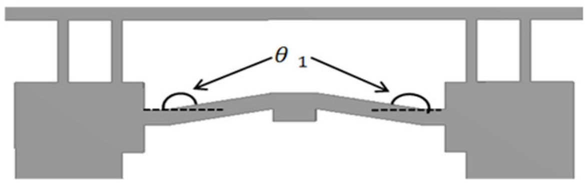

(a) Y axis motion bridge

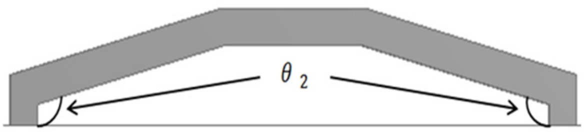

(b) Half bridge

Fig. 5. Optimization Factor

the critical design factor α (Eq. 8) for each bridge structure are chosen as the optimization variables. Optimization is divided into a two-step process where θ_1 of the bridge moving in the y-axis is optimized first, then θ_2 of the bridge moving in the z-axis is

optimized next. The range of variables θ_1, θ_2 are set to,

$$155° < \theta_1 < 175° \tag{9}$$

$$94.5° < \theta_2 < 115.5° \tag{10}$$

Where the maximum of θ_1 and the minimum of θ_2 were each set near angles that render a flat bridge structure. The minimum of θ_1 and the maximum of θ_2 were set heuristically so that the total range would be approximately 20 degrees. The output variable is the maximum displacement of the stage structure. The input value is set at 20 μm according to the specification of the piezo-element to be used in the experiment (Table 1).

3.2 Simulation

Fig. 6 and Fig. 7 show the response surface analysis for the variables θ_1, θ_2 where the results are almost identical for both Al 7075-T6 and ABS. Both materials have a motion amplification ratio of 4.0. Also for both materials, the maximum displacement for θ_1 occurs between 165° and 170° and for θ_2 occurs between 100° and 105°. Based on these simulation results, the values chosen for θ_1, θ_2 are 168.1 and 101.0 respectively for designing the motion stage.

Table 1. Piezo Specification

NAC2015-H16-A01(Noliac)	
Dimension	10 mm10 mm16 mm
Free Stroke	21 μm (0V - 150V)
Stiffness	1400 N/um
Capacitance	4790 nF
Blocking Force	4200 N

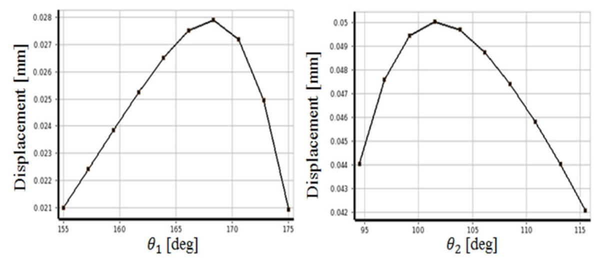

Fig. 6. Response surface of Al 7075-T6

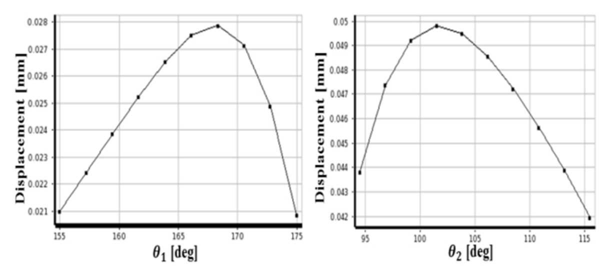

Fig. 7. Response surface of ABS

Table 2. Optimization result

Parameters	Al 7075-T6	ABS
Displacement [mm]	0.0498	0.0496
Stress [MPa]	135.79	4.36

Table 2 shows the results of the response surface analysis. Although the displacements for Al 7075-T6 and ABS are almost identical, note that the stress level of

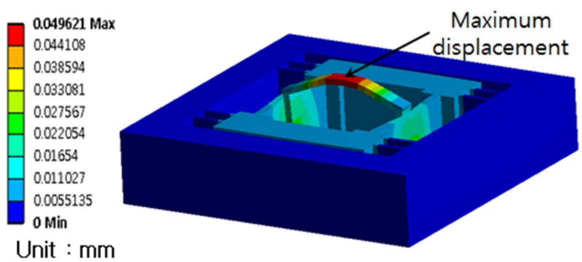

Fig. 8. Maximum Displacement

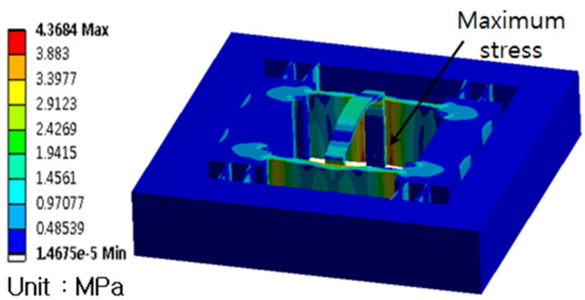

Fig. 9. Maximum Stress

the ABS is approximately 31 times lower. The yield stress for Al 7075-T6 and ABS are respectively 570 MPa, 40 MPa. Therefore, the simulation results for stress are each 4.1 vs 9 times smaller than the yield stress for Al 7075-T6 and ABS. This shows that ABS material compared to Al 7075-T6 is less restricted due to stress in designing flexure structures.

Fig. 8 and Fig. 9 each show the maximum displacement and maximum stress simulation results for the ABS material.

4. Experimental Results

4.1 Experiment Description

Based on the optimization results presented in Section 3, a Vertical micro-positioning stage has been fabricated using a 3D printer with ABS material. The stage is shown in Fig. 10. The 3D printer used is the Projet® 5000(3D Systems), which uses the MJM (Multi-Jet Modeling) method. MJM method sprays a photopolymer resin and wax from the printer head followed by a UV light which

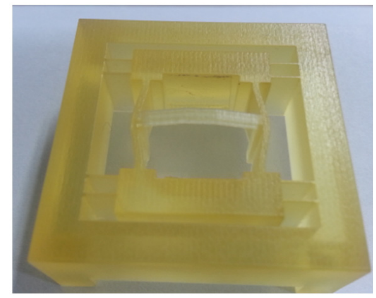

Fig. 10. Image of 3D printed Motion Stage (ABS material)

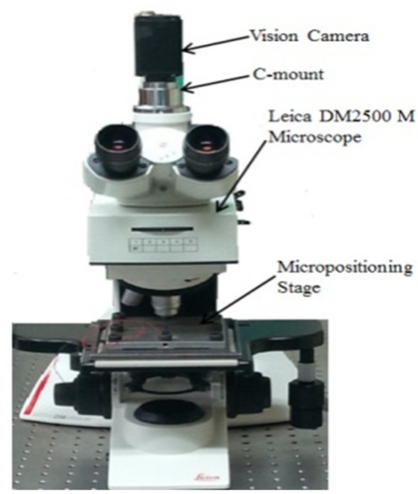

Fig. 11. Microscope used for displacement measurement

hardens the structure in layers. This 3D printer has maximum fabrication volume of this device is 550 × 393 × 300 mm, 0.025-0.05 mm precision, 375× 375 × 790 DPI (xyz) in HD mode, a minimum layer thickness of 32 μm. This resolution is sufficient to manufacture our motion stage.

The measurement of the vertical motion was performed using an interference microscope as shown in Figure 11. In order to measure vertical motion, the method developed by Kim et. al [13,14] was employed. The measurement method measures the movement of interference fringes using a CCD camera to estimate the vertical motion of the motion stage. Fig. 12 shows the flow diagram of the measurement process which is implemented in Labview. First, the fringe image model $M_i(x, y)$ is defined. As the stage moves, the image of the stage I(x, y) is obtained.

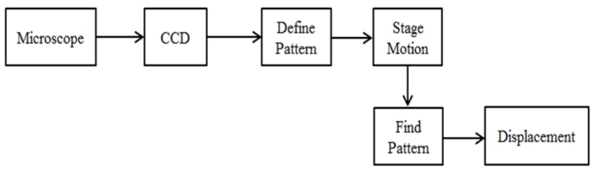

Fig. 12. Microscope used for displacement measurement

Table 3. Experimental results

Voltage [V]	Piezo [μm]	End Effector [μm]	Amplification Ratio
5	0.98	3.90	3.98
10	2.12	8.54	4.03
15	3.33	13.4	4.07
20	4.55	18.71	4.11
25	5.79	23.76	4.10
30	7.00	28.74	4.11
35	8.12	33.47	4.12
40	9.21	37.85	4.11

The model is found in the image using the correlation function,

$$r(u,v) = \frac{\Sigma I(x,y) M_i(x-u,y-v) - \bar{I}\cdot\overline{M_i}}{\sqrt{[I(x,y)^2 - \bar{I}^2]\cdot[\Sigma M_1(x-u,y-v)^2 - \overline{M}_i^2]}} \tag{11}$$

and the position $(\hat{x}_1, \hat{y}_1)$ of the model is found where,

$$r(\hat{x}_1, \hat{y}_1) = \max\{r(u,v)\} \tag{12}$$

Further details of the measurement method can be found in the literature [13].

4.2 Experiment Results

The input voltage to the piezo-element was varied from 0 to 40 V in 9 steps while the displacement of the end-effector, i.e. the half bridge, was measured. The experimental results are shown in Table 3. Amplification ratio is approximately 4 which agree with the simulation results. Fig. 13 plots the applied input voltage vs piezo-element displacement while Fig. 14 plots input voltage vs end effecter displacement.

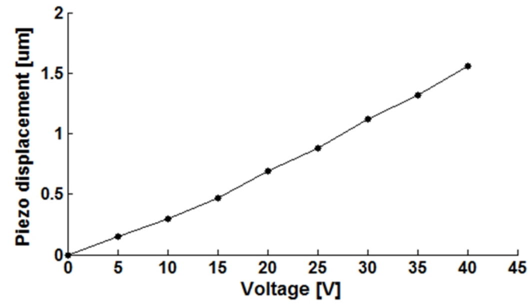

Fig. 13. Piezo displacement

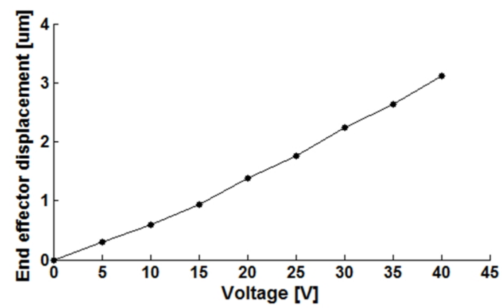

Fig. 14. End effector displacement

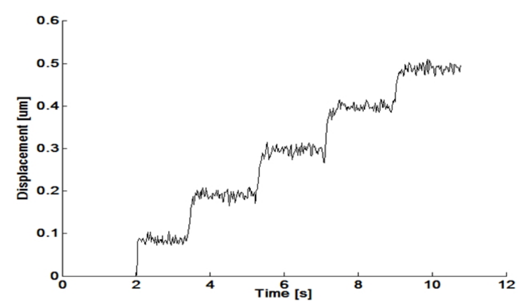

Fig. 15. 100nm Stepping

In order to test the performance of the motion stage, 100 nm step inputs were applied to the stage (see Fig. 15). Measurement noise in the interference microscope is currently approximately 10 nanometers which attribute to the noise at each step. Furthermore, a gradual drift can also be seen at each step. It is thought that in the future improving the CCD camera performance and introducing further feedback control can improve motion control performance. Utilizing the motion measurement as feedback for close-loop control could especially correct for drift and non-linearity.

5. Conclusion & Remarks

This paper presented the development of a piezo-driven vertical micro-positioning stage fabricated with a 3D printer using ABS material. Two bridge structures were constructed which amplified and transferred the horizontal motion of the piezo-element into vertical motion of the end-effector. It was shown that the use of 3D printed ABS material for creating flexure motion stages has less restriction on stress compared to traditional material. Compared to previous materials, the stage structure exhibits significantly less structural stress which allows for more freedom of design. Furthermore, the required force to actuate the motion stage decreases which relaxes power requirements for the piezoelectric element. Overall, we have the demonstrated the future possibilities of applying 3D printers and ABS material in fabricating linear driven motion stages. Due to the many advantages of 3D printing technology, various motion stage designs having multiple degrees-of-freedom and larger motion amplification should be possible.

References

[1] B.H. Kang, J.T.Y. Wen, N.G. Dagalakis, and J.J. Gorman, "Analysis and Design of Parallel Mechanisms With Flexure Joints," IEEE Transactions On Robotics, vol. 21, no. 6, pp. 1179-1185, 2005.

[2] S.B. Choi, S.S. Han, and Y.S. Lee, "Fine Motion Control of a Moving Stage using a Piezo-actuator Associated with a Displacement Amplifier," Smart Mater. Struct., vol. 14, no. 1, pp. 222-230, 2005.

[3] H.W. Ma, S.M. Yao, L.Q. Wang, Z. Zhong, "Analysis of the displacement amplification ratio of bridge-type flexure hinge,"Sensors and Actuators, A 132, pp. 730-736, 2006.

[4] J.H. Kim, S.H. Kim, and Y.K. Kwak, " Development and optimization of 3-D bridge-type hinge mechanisms," Sensors and Actuators, A 166, pp. 530-538, 2004.

[5] J.S. Kim and M.Y. Yang, "Design of 3-DOF (Z-translation, Pitch, Roll motion) precise tilt table for a large surface workpiece with micro features to compensate set-up," J. of KSMT Fall Conference, pp. 28-33, 2006.

[6] P. Gao, S.M. Swei, and Z. Yuan, "A New Piezo-driven Precision Micro-positioning Stage utilizing Flexure Hinges," Nanotechnology, vol. 10, no. 4, pp.394-398 , 1999.

[7] T.F. Lu, D.C. Handley, Y.K. Yong, and C. Eales, "A Three-DOF Compliant Micro-motion Stage with Flexure Hinges," Ind. Robot, vol. 31, no 4, pp. 355-361, 2004.

[8] K. Hu, J.H. Kim, J. Schmiedeler, and C.H. Menq, "Design, Implementation, and Control of a Six-Axis Compliant Stage," Rev. Sci. Instrum., vol. 79, paper no. 025105, 2008.

[9] K.H. Kwak and S.W. Park, "Global 3D Printer Industry Technology Trends Analysis," J. of the KSME, vol. 53, no. 10, pp. 58-64, 2013.

[10] J.H. Rho, S.K. Jeng, M.H. Kwak, and D.H. Lee, "Rapid Prototyping with Vehicle Modeling Function and 3D Printer," Proc. of KSAE Annual Conference, pp. 2541-2544, 2009.

[11] H.C. Kim, S. Lee, and S.H. Lee, "Rapid Tooling Technology for Producing Functional Prototypes using Ceramic Shell Investment Casting and Patterns Produced Directly from ThermoJet 3D printer," J. Kor. Soc. Precis. Eng., vol. 23, no. 8, pp. 203-210, 2006.

[12] H.J. Jung and J.H. Kim, "Fabrication of Piezo-Driven Micro-positioning Stage using 3D printer," J. of KSPE, vol. 31, no. 3, pp. 277-283, 2014.

[13] Jung H. Kim and C.-H. Menq, "Visually Servoed 3-D Alignment of Multiple Objects with Sub-nanometer Precision," IEEE Trans. on Nanotechnology, vol. 7, no.3, May 2008

[14] Jung H. Kim," Emulation of Anti-alias Filtering in Vision Based Motion Mmeasurement," Journal of Korea Robotics Society, vol. 6, no. 1, pp. 18-26.

[15] C.W. Park, J.B. Lee, B.S. Kim, J.S. Park, H.G. Sung," The Development of High Precision Manipulator and Micro Gripper," Journal of Korea Robotics Society, vol. 2, no. 1, pp. 64-70

김 정 현

1999 서울대학교 컴퓨터공학과(공학사)

2003 Ohio State University, Dept. Mechanical Eng. (석사)

2007 Ohio State University, Dept. Mechanical Eng. (박사)

2008 ~ 2010 미 Lam Research Corp. 근무

2010 ~ 현재 경성대학교 메카트로닉스공학과에서 교수로 근무

관심분야: 정밀계측, Fault Detection Diagnosis